

Noise-enhanced quantum transport on a closed loop using quantum walks

C.M. Chandrashekar^{1,2,*} and Th. Busch^{1,2,†}

¹*Physics Department, University College Cork, Cork, Ireland*

²*Quantum Systems Unit, Okinawa Institute of Science and Technology, Okinawa, Japan*

We study the effect of noise on the transport of a quantum state on a closed loop. Using a discrete-time quantum walk dynamics, we demonstrate that the transport efficiency is enhanced with noise when the number of sites in the loop is small and suppressed when the number of sites in the loop grows. By using the concept of measurement induced disturbance we identify the regimes in which genuine quantum effects are responsible for the enhanced transport.

I. INTRODUCTION

Studying energy transfer or transport efficiencies in the presence of quantum coherence has recently become an active area due to its applications in many different scientific fields. A number of microscopic models have been developed and their studies highlight the possibility of quantum coherence playing an important role in, for example, the energy transfer process in mesoscopic bio-chemical systems [1–7]. At the same time, first experimental studies have shown that quantum coherence can play a significant role in photosynthetic light-harvesting complexes [8–10] and in chromophoric energy transport [11]. Since one of the main results in many of these studies is the enhancement of the transport efficiency in the presence of noise [6–8, 12, 13], it becomes clear that understanding the dynamics of noisy quantum state transport can play a significant role in modeling and understanding natural physical and bio-chemical processes. Identifying models and dynamics in which the effect of the noise contributes constructively to transport efficiency is therefore an important task. While the dynamics of quantum systems can be described by different forms of evolution, here we concentrate on quantum walks, which have been shown to be an effective model to understand, for example, photosynthetic energy transfer [8, 13].

Quantum walks evolve a particle in a series of superposition in position space [14–18] and are the quantum analogue to classical random walks. Over the past decade, quantum walks have emerged as an efficient tool to develop quantum algorithms [19, 20], to have coherent control of atoms and Bose-Einstein condensates in optical lattices [21, 22], to create topological phases [23], to construct protocols for quantum state transfer [24, 25], and to generate entanglement [26] among many other applications. Quantum walks are therefore well suited to serve as a framework to simulate, control and understand the dynamics of physical and bio-chemical systems [27].

Many organic and bio-chemical systems can be modeled by considering a closed loop of n sites, which has

connections to other systems at specific positions. To measure the transport efficiency resulting from a discrete-time quantum walk on such a system [28–30] we designate one of the sites as a sink at which the amplitude of the particle gets absorbed and might, for example, be transported to a neighboring loop or network. Since this is a periodic system it is clear that for infinitely long times 100% of the wavefunction will be absorbed at the sink, however the efficiency at short times will depend strongly on the sink's position as well as the interaction with the environment. By modeling the strength of the environmental effects using a depolarizing and a dephasing channel, we find that an enhancement of state transport can be seen when the number of sites in the closed loop is small for any level of noise. With an increased number of sites, however, a suppression is seen. Studying the transport efficiency as a function of time we also identify regimes in which temporal enhancement can be found. To determine the quantumness of the transport we use measurement induced disturbance [31, 32] and highlight the regime where the quantum correlations and enhancement of transport coexist. Along with helping to understand and model the energy transfer and state transport process in naturally occurring system, the recent experimental progress in creating quantum walks in various physical systems (NMR [33–35], cold ions [36, 37], photons [38–43], and ultracold atoms [44]) allow to study and engineer transport process in laboratory.

In Section II we define the discrete-time quantum walk model used to describe the evolution process and transport efficiency. In Section III the effects of depolarizing and dephasing noisy channels on the transport process are discussed and in Section IV we use measurement induced disturbance to measure the quantum correlations in the transport process. We highlight the regime in which quantumness and efficient transport coexist and conclude in Section V.

II. MODEL, EVOLUTION PROCESS AND TRANSPORT EFFICIENCY

We will denote the wavefunction of the particle on the loop as $|\Psi(t)\rangle = \sum_j |\psi(j, t)\rangle$, where the $\psi(j, t)$ represent two-component amplitude vectors of the particle at po-

*Electronic address: cmadaiah@phys.ucc.ie

†Electronic address: thbusch@phys.ucc.ie

sition j and time t ,

$$|\psi(j, t)\rangle = (c_1|\downarrow\rangle + c_2|\uparrow\rangle) \otimes |j, t\rangle = \begin{bmatrix} \psi_L(j, t) \\ \psi_R(j, t) \end{bmatrix}. \quad (1)$$

Here L indicates the left-moving component and R the right-moving one. The position space for the particle to move in is a closed loop with n discrete sites, $j = 1, \dots, n$, and we choose the initial wave function to be localized at $j = 1$ and $t = 0$ as

$$|\psi(1, 0)\rangle = \frac{1}{\sqrt{2}}(|\downarrow\rangle + |\uparrow\rangle) \otimes |1, 0\rangle. \quad (2)$$

After an evolution for time t with equal left- and right-moving components the particle's state will evolve into

$$|\Psi(t)\rangle = \sum_j |\psi(j, t)\rangle = \sum_j \begin{bmatrix} \psi_L(j, t) \\ \psi_R(j, t) \end{bmatrix} = W^t \begin{bmatrix} \psi_L(1, 0) \\ \psi_R(1, 0) \end{bmatrix}, \quad (3)$$

where

$$W = \frac{1}{\sqrt{2}} \begin{bmatrix} a^\dagger & -ia^\dagger \\ -ia & a \end{bmatrix}, \quad (4)$$

and the action of the operators a and a^\dagger on $\psi_{L(R)}(j, t)$ are given by

$$a\psi_{L(R)}(j, t) = \psi_{L(R)}((j+1) \bmod(n+1), t+1), \quad (5a)$$

$$a^\dagger\psi_{L(R)}(j, t) = \psi_{L(R)}((j-1) \bmod(n+1), t+1). \quad (5b)$$

The wavefunction of the particle at each position j is therefore given by

$$\begin{bmatrix} \psi_L(j, t+1) \\ \psi_R(j, t+1) \end{bmatrix} = \frac{1}{\sqrt{2}} \begin{bmatrix} a & -ia^\dagger \\ -ia & a^\dagger \end{bmatrix} \begin{bmatrix} \psi_L(j, t) \\ \psi_R(j, t) \end{bmatrix}, \quad (6)$$

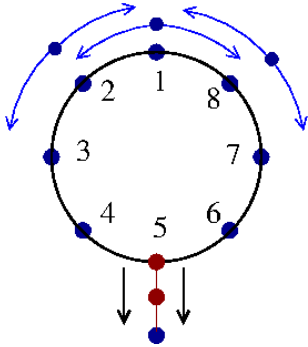


FIG. 1: (Color online) (a) Schematic of a closed loop with 8 sites and sink potential at site number 5. Depending on the value of sink potential, a complete ($r = 1$) or a fractional transfer ($r < 1$) of state is observed.

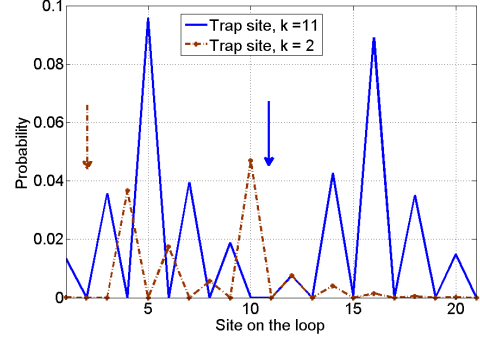


FIG. 2: (Color online) Probability distribution of state in a closed loop of 21 sites at $t = 25$. Left and right end sites in the plots are connected in the loop. The strength of the sink potential is $r = 1$ and the sink is the nearest ($k = 2$) or the farthest ($k = 11$) neighbor to the initial position. For $k = 2$ the large fraction of the amplitude fall into the sink very soon with only a small fraction moving towards the site 21 and eventually to the sink. Whereas, for $k = 11$, equal contributions of the clockwise and anticlockwise moving parts of the amplitude to the sink can be seen.

which leads to

$$\psi_L(j, t+1) = \frac{1}{\sqrt{2}} \left[\psi_L((j+1) \bmod(n+1), t) - i\psi_R((j-1) \bmod(n+1), t) \right], \quad (7a)$$

$$\psi_R(j, t+1) = \frac{1}{\sqrt{2}} \left[\psi_R((j-1) \bmod(n+1), t) - i\psi_L((j+1) \bmod(n+1), t) \right]. \quad (7b)$$

To quantify the efficiency of the transport, we will consider one position k on the closed loop to act as a sink (position 5 in Fig. 1). Depending on the strength of the sink potential r ($0 \leq r \leq 1$), a certain fraction of the wave amplitude is transported to the sink (neighboring loop/network) and the transport efficiency (TE) at any time t will be

$$TE = 1 - \sum_{j=1}^n \langle \psi(j, t) | \rho(t) | \psi(j, t) \rangle, \quad (8)$$

where

$$\begin{aligned} \rho(t) &= (\mathbb{1}_2 \otimes s_k) W \rho(t-1) W^\dagger (\mathbb{1}_2 \otimes s_k)^\dagger \\ &= S_k W \rho(t-1) W^\dagger S_k^\dagger \end{aligned} \quad (9)$$

and S_k is a $n \times n$ unity matrix in which 1 is replaced by $1 - r$ at position (k, k) . The left and the right moving components at position $(k \pm 1) \bmod(n+1)$ are given by

$$\psi_L((k+1) \bmod(n+1), t+1) = \frac{1}{\sqrt{2}} \left[\psi_L((k+2) \bmod(n+1), t) - i\sqrt{1-r} \psi_R(k, t) \right], \quad (10a)$$

$$\psi_R((k+1) \bmod(n+1), t+1) = \frac{1}{\sqrt{2}} \left[\sqrt{1-r} \psi_R(k, t) - i\psi_L((k+2) \bmod(n+1), t) \right], \quad (10b)$$

$$\psi_L((k-1) \bmod(n+1), t+1) = \frac{1}{\sqrt{2}} \left[\sqrt{1-r} \psi_L(k, t) - i\psi_R((k-2) \bmod(n+1), t) \right], \quad (10c)$$

$$\psi_R((k-1) \bmod(n+1), t+1) = \frac{1}{\sqrt{2}} \left[\psi_R((k-2) \bmod(n+1), t) - i\sqrt{1-r} \psi_L(k, t) \right]. \quad (10d)$$

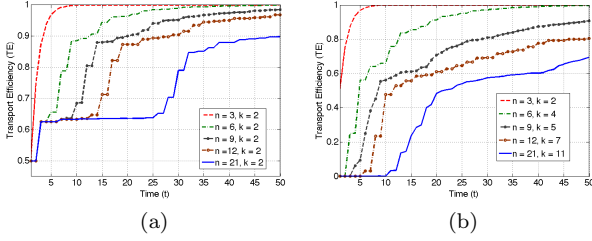


FIG. 3: (Color online) Transport efficiency as a function of time on a closed loop with different number of sites (n) when the sink potential $r = 1$ is located at (a) the site nearest to the initial side and (b) furthest from the initial side. Note the different axis scalings.

When sink potential has maximum strength ($r = 1$), the right hand side of the preceding expression will have only one term which describes a complete absorption of the amplitude into the site k , suppressing the interference of the clockwise and counter-clockwise moving parts of the amplitude. In this case the evolution is identical to one along a line with sink at the extreme ends. In Fig. 2, the probability distributions for a state on a closed loop of 21-sites with the sink potential $r = 1$ at sites $k = 2$ and $k = 11$ when $t = 25$ is shown. When the sink is the nearest neighbor to the initial position, 50% of the amplitude gets absorbed at $t = 1$ and therefore no longer contributes to the interference of the state at time $t > 1$. The fraction of the amplitude surviving continues to evolve in a superposition towards and away from the sink as time progresses. This quickly reduces the fraction of the amplitude remaining further for the evolution when the loops are small (see Fig. 3a). When the sink is the farthest site from the initial position in the loop, the interference results in the well known fast spreading of the amplitude around the loop before it reaches the sink. This results in an initially slower transfer of amplitude into the sink which leads to an overall slower rate of absorption into the sink even for long times (see Fig. 3(b)).

For $r < 1$ a fraction of the amplitude ($\sqrt{1-r}$) getting into the sink is retained in the loop and continues to evolve and contribute to the interference. In Fig. 4, we

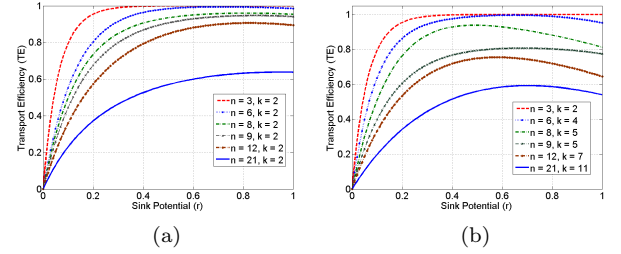


FIG. 4: (Color online) Transport efficiency at time $t = 25$ on a closed loop with different sink potential r . (a) When sink is the nearest neighbor (site 2) of the initial site. (b) When sink is the farthest site from the initial site.

show the transport efficiency as a function of the sink potential strength r . When sink is the nearest neighbor, a steep increase in the transport efficiency is seen for small values of r , which becomes less pronounced with increasing loop size [Fig. 4(a)]. A similar behavior is found when the sink is farthest site from the initial position, however the curves also show a local maximum for a value of $r < 1$ [Fig. 4(b)]. The decrease beyond the maximum is stronger for loops with an even number of sites and can be attributed to the symmetric interference of the left and right moving components, resulting in a larger transfer of state when $r < 1$.

III. DECOHERENCE

Let us now introduce a noisy environment and discuss its effects on the transport efficiency. The standard ways to introduce decoherence into quantum systems are to use a depolarizing and a dephasing channel, which correspond to noise sources affecting the amplitude and the phase of the particle.

A. Depolarizing channel

A depolarizing noise channel replaces the density matrix of a two-state system by a linear combination of a

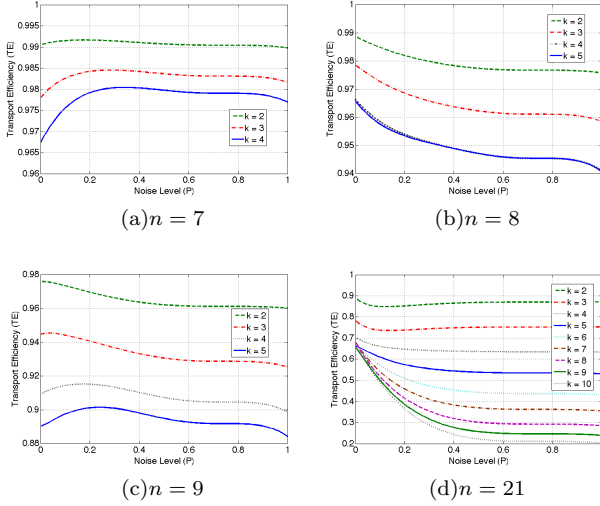


FIG. 5: (Color online) Transport efficiency subject to a depolarizing noise channel on a closed loop of (a) 7 sites (b) 8 sites (c) 9 sites and (d) 21 site after $t = 40$ with $r = 0.8$. Note different axis scalings.

completely mixed state and the unchanged state

$$\rho(t) = S_k W \left[(1 - P)\rho(t-1) + \frac{P}{3} \left(\mathbb{X}\rho(t-1)\mathbb{X}^\dagger + \mathbb{Y}\rho(t-1)\mathbb{Y}^\dagger + \mathbb{Z}\rho(t-1)\mathbb{Z}^\dagger \right) \right] W^\dagger S_k^\dagger, \quad (11)$$

where $\mathbb{X} = \sigma_1 \otimes \mathbb{1}$, $\mathbb{Y} = \sigma_2 \otimes \mathbb{1}$ and $\mathbb{Z} = \sigma_3 \otimes \mathbb{1}$ with σ_1 , σ_2 , and σ_3 being the standard Pauli operators.

Considering initially the system in the absence of noise, we show in Fig. 4(a) the situation when the sink, k , is the nearest neighbor to the initial position and find that the transport efficiency reaches maximum value for $r < 1$ and remains close to the maximum value for $r = 1$. When the sink is furthest away from the initial position, the maximum value is also reached for $r < 1$, however we observe a stronger decline for $r = 1$, see Fig. 4(b). The influence of noise is displayed in Figs. 5 and 6 for $r = 0.8$ and $r = 1$, respectively, and shows a complex behavior. For a loop of 7 sites (see Figs. 5(a) and 6(a)) a clear increase in transport efficiency can be seen for any value of the noise, however for the case of $n = 8$ we find a decrease for $r = 0.8$ independent of the position of the sink (see Fig. 5(b)), but an increase for large distances of the sink in the case of $r = 1$ (see Fig. 6(b)). When $n = 9$, with increase in the distance between the sink and the initial position, an initial increase in transport efficiency seen for small noise decreases with further increase in noise for $r = 0.8$ (see Fig. 5(c)). Whereas, an increase in transport efficiency with noise is seen for $r = 1$ (see Fig. 6(c)) but the trend in the way transport efficiency varies with

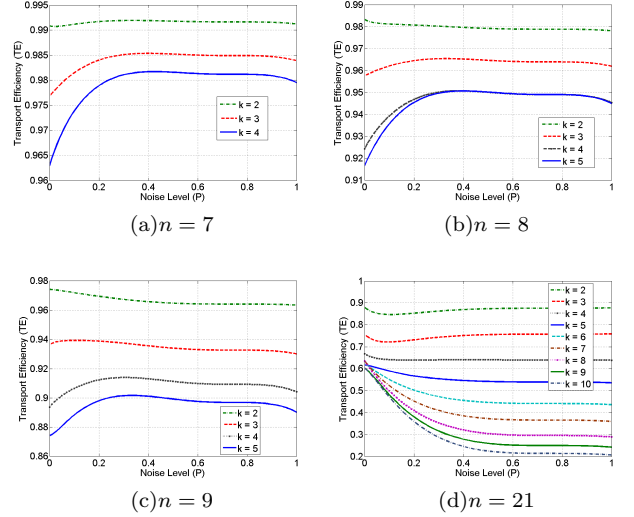


FIG. 6: (Color online) Transport efficiency subject to a depolarizing noise channel on a closed loop of (a) 7 sites (b) 8 sites (c) 9 sites and (d) 21 site after $t = 40$ with $r = 1$. Note different axis scalings.

noise is identical for both, $r = 0.8$ and $r = 1$. With increase in loop size and the distance between the initial position and sink, decrease in the transport efficiency is seen for all r (see Fig. 5(d) and Fig. 6(d)). The general trend when n is small and odd is, the transport efficiency with noise scales up with increase in r . When n is small and even, the transport efficiency with noise when $r = 1$ shows an inverse trend compared to the transport efficiency for $r = 0.8$. For even n and $r < 1$, along with the interference due to the evolution process, interference between clockwise and counter-clockwise traveling parts of the wavefunction in the loop happens at site 1 and $(\frac{n}{2} + 1)$. When n is odd and $r < 1$, interference due to clockwise and counter-clockwise traveling parts happens only at site 1.

The detailed transport efficiency on 8-site loop for a sink potential $r = 1$ when at $k = 2$ and $k = 5$ is shown in Fig. 7 for different times t . At short times a small enhancement of the transport efficiency can be seen if the sink distance is small (see Fig. 7(a) for $t = 10$) but for longer times the noise has only a very small and ultimately negligible effect on the transport efficiency (see Fig. 7(c)), because large fraction of the amplitude is transferred to the sink before the depolarizing noise can affect the dynamics of the transport process. Conversely, when $k = 5$ the suppression of the transport efficiency seen for $t = 10$ (Fig. 7(b)) changes to an enhancement for longer times t (Fig. 7(d)). This is also consistent with the behavior shown in Fig. 6(b) for $k = 4$ and $k = 5$, respectively. The reason for this can be found in the fact that the noise alters the ballistic-like dynamics of the initially Gaussian state [28]. If the sink is far away from the initial state and the loop only has a small number of

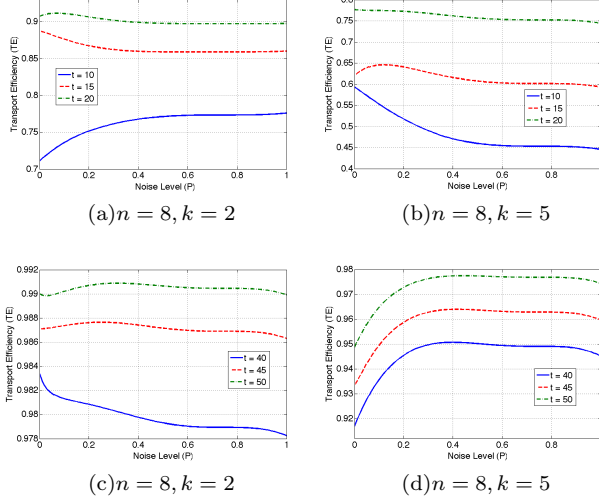


FIG. 7: (Color online) Transport efficiency as a function of depolarizing noise for $r = 1$ for different times $t = 10$, $t = 15$, $t = 20$, [(a) and (b)], $t = 40$, $t = 45$, and $t = 50$ [(c) and (d)]. Note different axis scalings.

sites ($n = 7, 8, 9$), the fraction of the amplitude that has reached the sink for short times ($t = 10$) is smaller than in the absence of noise, leading to a decrease in transport efficiency with an increase in noise. For longer times the Gaussian-like distribution also moves towards the sink, which in small loops results in a small enhancement in transport efficiency. For loops with large number of sites, however, the effect of noise dominates completely over the ballistic transport, which results in a distribution centered around the initial position, which only slowly reaches the sink and in turn results in strong degradation of the transport efficiency (see Fig. 6(d)).

B. Dephasing channel

The density matrix of a two-state particle in the above system when subjected to a dephasing channel will be given by

$$\rho(t) = S_k W [P \mathbb{E} \rho(t-1) \mathbb{E}^\dagger + (1-P) \rho(t-1)] W^\dagger S_k^\dagger, \quad (12)$$

where

$$\mathbb{E} = |\uparrow\rangle\langle\uparrow| + e^{-i\delta} |\downarrow\rangle\langle\downarrow|, \quad (13)$$

and P and δ are the dephasing noise level and angle, respectively. For $\delta = 0$, \mathbb{E} is identity corresponding to a noiseless evolution and for $\delta = \pi$, \mathbb{E} represents a phase flip channel.

In Fig. 8 we show the transport efficiency as a function of δ for different noise levels P for an 8-site loop with the sinks at $k = 2$ and $k = 5$ for a time $t = 40$ when

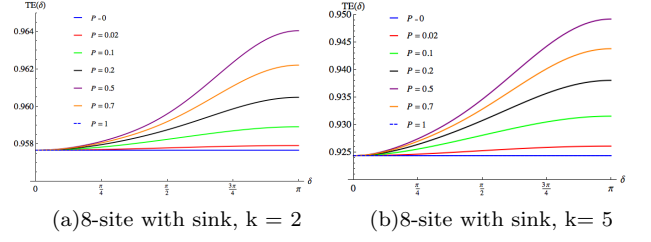


FIG. 8: (Color online) Transport efficiency with sink at position (a) 2 and (b) 5 on an 8-site ring as a function of δ for different dephasing noise level at $t = 40$. For any non-zero noise level transport efficiency is maximum for $\delta = \pi$.

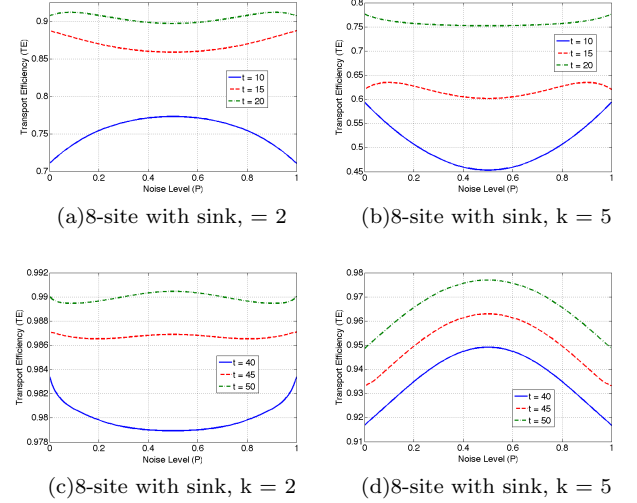


FIG. 9: (Color online) Transport efficiency of two-state particle with dephasing noise with $\delta = \pi$ on a 8-site ring with the sink, $k = 2$ and $k = 5$ at $t = 10$, $t = 15$, $t = 20$, [(a) and (b)], $t = 40$, $t = 45$, and $t = 50$ [(c) and (d)].

sink potential is $r = 1$. One can clearly see an increase in the transport efficiency in the presence of depolarizing noise, which gets more pronounced the larger the noise and the dephasing angle. However, the difference between the maximum and the minimum of the transport efficiency is very small and given by 0.6% when the trap site is the nearest neighbor and 2.5% when the trap site is the farthest from the initial position. In Fig. 9 we show the effect of the dephasing channel for fixed $\delta = \pi$ for different values of t . When the sink is the nearest neighbor to the initial position, the enhancement of the transport efficiency seen for $t = 10$ (Fig. 9(a)) changes into a suppression for increasing values of t (Fig. 9(c)). Conversely, when the sink is farthest away to the initial position ($k = 5$ for $n = 8$), the suppression of transport efficiency seen for $t = 10$ (Fig. 9(b)) slowly changes into an enhancement for longer times (Fig. 9(d)). The effects of a dephasing noisy channel are therefore very similar

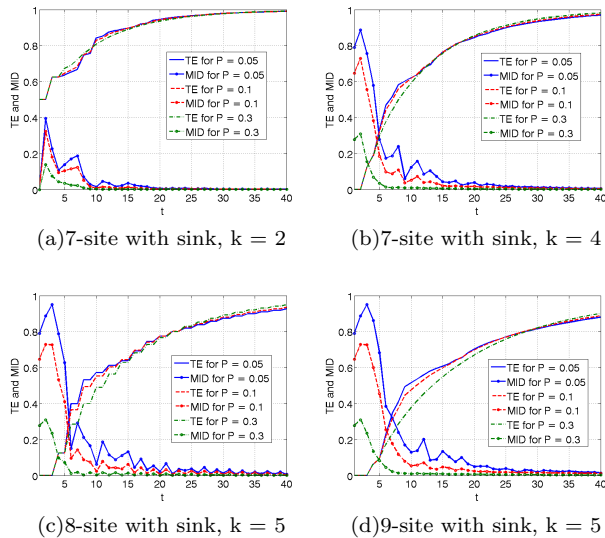


FIG. 10: (Color online) Transport efficiency of two-state particle and quantum correlations between the particle and the ring when subjected to the decoherence due to depolarizing channel with time t on (a) 7-cycle with sink, $k = 2$ (b) 7-cycle with sink, $k = 4$ (c) 8-cycle with sink at position 5 (d) 9-cycle with sink, $k = 5$.

to the effects due to depolarizing noisy channel discussed in the preceding section with one major difference. That is, unlike the depolarizing noisy channel, the extrema for the transport efficiency for the dephasing channel are achieved at $P = 0.5$ [28]. This is due to a symmetry of the quantum walk which holds for dephasing channel and not for the depolarizing channel. Symmetry of quantum walk can be defined as an addendum of operations resulting in the identical probability distribution. When $P = 1$ and $\delta = \pi$ in Eq.(12) the evolution is identical to the phase flip operation during each step of the quantum walk evolution and the resulting probability distribution is identical to the noiseless evolution, therefore, we can call this as a symmetry of the quantum walk due to the addendum of phase flip channel [28]. Therefore, for evolution with dephasing noisy channel, with increase in P , a maximally mixed state $\rho(t)$ is obtained for $P = 0.5$. Whereas, the symmetry of the quantum walk does not hold for addendum of depolarizing noisy channel and a maximally mixed state $\rho(t)$ in Eq.(11) is obtained only when $P = 1$.

IV. QUANTUMNESS IN THE TRANSPORT PROCESS

Let us finally discuss the quantum nature of the decoherence-influenced quantum walks we have presented, to allow us to identify the importance of quantum correlation in the regimes of transport enhancements. To

quantify this we will make use of the concept of measurement induced disturbance (MID) [32] as a measure of quantum correlations between the closed loop with the sink and the surviving part of the particle state as the subsystems.

The quantum correlations of the bipartite state ρ living in the Hilbert space $\mathcal{H}_A \otimes \mathcal{H}_B$ can be obtained by using the reasonable measure of total correlations and subtracting a reasonable measure of classical correlations present in ρ . If the reduced density matrices are denoted by ρ_A and ρ_B , a reasonable measure of total correlations between systems A (closed loop) and B (particle) is the mutual information, given by

$$I(\rho) = S(\rho_A) + S(\rho_B) - S(\rho), \quad (14)$$

where $S(\rho) = -\text{Tr}(\rho \ln \rho)$ denotes the von Neumann entropy. By taking the complete projective measurement $\Pi_A \otimes \Pi_B$ determined by the eigen-projectors Π_A^i and Π_B^i of the marginal states $\rho_A = \sum_j p_A^j \Pi_A^j$ and $\rho_B = \sum_j p_B^j \Pi_B^j$, where p_A and p_B are the corresponding eigenvalues, we can define the MID as

$$Q(\rho) = I(\rho) - I[\Pi(\rho)], \quad (15)$$

where

$$\Pi(\rho) \equiv \sum_{j,k} \Pi_A^j \otimes \Pi_B^k \rho \Pi_A^j \otimes \Pi_B^k \quad (16)$$

is the post-measurement state after local measurements Π_A and Π_B . The state $\Pi(\rho)$ may be considered classical in the sense that there is a (unique) local measurement strategy, namely Π , that leaves $\Pi(\rho)$ unchanged. This strategy is special in that it produces a classical state in ρ while keeping the reduced states invariant. If we accept that $I[\Pi(\rho)]$ is a good measure of *classical* correlations in ρ , then one can consider MID as a computable measure of quantum correlation [32].

In absence of noise, quantum correlations between the loop and the particle vanish only when the particle is completely transported to the sink, that is, transport efficiency is one ($\text{TE}=1$). With noise, quantum correlations vanish before the state is completely transported to the sink. In Fig. 10, we show the transport efficiency and the corresponding quantum correlations using MID as a function of time for different depolarizing noise levels. One can see that even a small increase in the noise level leads to a significant decrease in the strength of the quantum correlations and they vanish even before the transport efficiency gets close to one. This shows that the quantum correlations are only present for a very short amount of time during the transport process. From Fig. 10, we can note that the quantum correlation during transport process on a loop of small size (7, 8, 9) reduces faster with time when the sink is nearest neighbour than when the sink is the farthest site. Therefore, from these observations we can say that the enhancement of transport efficiency is seen when the noise level is very small, sink

is nearest neighbor to the initial position, and time t is small. This is the regime where quantum correlations and enhancement of transport efficiency coexist.

In addition, if the sink of the loop is connected to second loop and if the quantum correlations between the surviving particle and the loop is non-zero, then non-zero quantum correlation between the second loop and the initial loop will be established.

V. CONCLUSION

Using a discrete-time quantum walk as a transport process we have studied the transport efficiency of a quantum state on a closed loop. In particular, we looked into the enhancement of quantum transport in presence of noise modeled using depolarizing and dephasing channel. We have shown that the noise channels can enhance the transport efficiency only when the number of sites in the closed loop is small. In addition, we have found enhancement for short times when the sink is the nearest neighbor of the initial site and for longer times t , when

the sink is farthest from the initial position.

An other important aspect we looked into is the loss of quantum correlations due to the presence of noise and we have identified regimes where the noise-enhanced transport and significant quantum correlations coexist. We have shown that only for small time t and when the sink is the nearest neighbor to the initial position, noise can enhance the quantum transport without destroying the quantum correlations in the process. This is an important result for example for systems in which energy or electrons are transferred from one loop or molecule to another, as it allows to generate quantum correlations between different loops or molecules.

Acknowledgments

We would like to acknowledge valuable discussions with J. Goold and R. Dornier. This project was supported by Science Foundation Ireland under Project No. 10/IN.1/I2979.

-
- [1] K.M. Gaab and C.J. Bardeen, *J. Chem. Phys.* **121**, 7813 (2004).
 - [2] A. Olaya-Castro, C. Lee, F. Olsen, and N. Johnson, *Phys. Rev. B*, **78**, 085115 (2008).
 - [3] P. Nalbach, J. Eckel, and M. Thorwart, *New J. Phys.*, **12**, 065043 (2010).
 - [4] P. Nalbach, D. Braun, and M. Thorwart, *Phys. Rev. E*, **84**, 041926 (2011).
 - [5] T. Scholak, F. Melo, T. Wellens, F. Mintert, and A. Buchleitner, *Phys. Rev. E*, **83**, 021912 (2011).
 - [6] P. Rebentrost, M. Mohseni, I. Kassal, S. Lloyd, and A. Aspuru-Guzik, *New J. Phys.* **11**, 033003 (2009).
 - [7] M. Plenio and S. Huelga, *New J. Phys.*, **10**, 113019 (2008).
 - [8] G. S. Engel, T. R. Calhoun, E. L. Read, T. Ahn, T. Manal, Y. Cheng, R. E. Blankenship, and G. R. Fleming, *Nature* **446**, 782-786 (2007).
 - [9] G. Panitchayangkoon, D. Hayes, K. A. Fransted, J. R. Caram, E. Harel, J. Wen, R. E. Blankenship, and G. S. Engel, *Proc. Natl. Acad. Sci.*, **107**, 12766 (2010).
 - [10] E. Collini, C. Y. Wong, K. E. Wilk, P. M. G. Curmi, P. Brumer, and G. D. Scholes, *Nature*, **463**, 644 (2010).
 - [11] P. Rebentrost, M. Mohseni, and A. Aspuru-Guzik, *J. Phys. Chem. B*, **113**, 9942 (2009).
 - [12] F. Caruso, A. W. Chin, A. Datta, S. F. Huelga, and M. B. Plenio, *J. Chem. Phys.*, **131**, 105106 (2009).
 - [13] M. Mohseni, P. Rebentrost, S. Lloyd, A. Aspuru-Guzik, *J. Chem. Phys.* **129**, 174106 (2008).
 - [14] G. V. Riazanov, *Sov. Phys. JETP* **6** 1107 (1958).
 - [15] R. Feynman, *Found. Phys.* **16**, 507 (1986).
 - [16] K. R. Parthasarathy, *Journal of Applied Probability*, **25**, 151-166 (1988).
 - [17] J. M. Lindsay and K. R. Parthasarathy, *Sankhyā: The Indian Journal of Statistics, Series A*, **50**, 151-170 (1988).
 - [18] Y. Aharonov, L. Davidovich and N. Zagury, *Phys. Rev. A* **48**, 1687, (1993).
 - [19] J. Kempe, *Contemp. Phys.* **44**, 307 (2003).
 - [20] A. Ambainis, *Int. Journal of Quantum Information*, **1**, No.4, 507-518 (2003).
 - [21] C. M. Chandrashekar and R. Laflamme, *Phys. Rev. A*, **78**, 022314 (2008).
 - [22] C. M. Chandrashekar, *Phys. Rev. A*, **83**, 022320 (2011).
 - [23] T. Kitagawa, M. S. Rudner, E. Berg, and E. Demler, *Phys. Rev. A* **82**, 033429 (2010).
 - [24] M. Christandl, N. Datta, A. Ekert, and A. J. Landahl, *Phys. Rev. Lett.*, **92**, 187902 (2004).
 - [25] P. Kurzyński and A. Wójcik, *Phys. Rev. A* **83**, 062315 (2011).
 - [26] Sandeep K. Goyal, C. M. Chandrashekar, *J. Phys. A: Math. Theor.* **43**, 235303 (2010).
 - [27] R. Dornier, J. Goold, and V. Vedral, *Interface Focus* **rsfs20110109** (2012).
 - [28] C. M. Chandrashekar, R. Srikanth, and S. Banerjee, *Phys. Rev. A*, **76**, 022316 (2007).
 - [29] Subhashish Banerjee, R. Srikanth, C. M. Chandrashekar, and Pranaw Rungta, *Phys. Rev. A*, **78**, 052316 (2008).
 - [30] C. Liu and N. Petulant, *Phys. Rev. E*, **81**, 031113 (2010).
 - [31] R. Srikanth, Subhashish Banerjee, and C. M. Chandrashekar, *Phys. Rev. A*, **81**, 062123 (2010).
 - [32] Luo, *Phys. Rev. A* **77** 022301 (2008).
 - [33] J. Du, H. Li, X. Xu, M. Shi, J. Wu, X. Zhou, and R. Han, *Phys. Rev. A* **67**, 042316 (2003).
 - [34] C. A. Ryan, M. Laforest, J. C. Boileau, and R. Laflamme, *Phys. Rev. A* **72**, 062317 (2005).
 - [35] D. Lu, J. Zhu, P. Zou, X. Peng, Y. Yu, S. Zhang, Q. Chen, and J. Du, *Phys. Rev. A* **81**, 022308 (2010).
 - [36] H. Schmitz, R. Matjeschk, Ch. Schneider, J. Glueckert, M. Enderlein, T. Huber, and T. Schaetz, *Phys. Rev. Lett.* **103**, 090504 (2009).

- [37] F. Zähringer, G. Kirchmair, R. Gerritsma, E. Solano, R. Blatt, and C. F. Roos, *Phys. Rev. Lett.* **104**, 100503 (2010).
- [38] H. B. Perets, Y. Lahini, F. Pozzi, M. Sorel, R. Morandotti, and Y. Silberberg, *Phys. Rev. Lett.* **100**, 170506 (2008).
- [39] A. Schreiber, K. N. Cassemiro, V. Potocek, A. Gabris, P. Mosley, E. Andersson, I. Jex, and Ch. Silberhorn, *Phys. Rev. Lett.*, **104**, 050502 (2010).
- [40] M. A. Broome, A. Fedrizzi, B. P. Lanyon, I. Kassal, A. Aspuru-Guzik, and A. G. White. *Phys. Rev. Lett.* **104**, 153602 (2010).
- [41] A. Peruzzo, M. Lobino, J. C. F. Matthews, N. Matsuda, A. Politi, K. Poullos, X. Zhou, Y. Lahini, N. Ismail, K. Wörhoff, Y. Bromberg, Y. Silberberg, M. G. Thompson, and J. L. O'Brien, *Science* **329**, 1500 (2010).
- [42] A. Schreiber, K. N. Cassemiro, V. Potocek, A. Gabris, I. Jex, and Ch. Silberhorn, *Phys. Rev. Lett.* **106**, 180403 (2011).
- [43] L. Sansoni, F. Sciarrino, G. Vallone, P. Mataloni, A. Crespi, R. Ramponi, and R. Osellame *Phys. Rev. Lett.* **108**, 010502 (2012).
- [44] K. Karski, L. Foster, J.-M. Choi, A. Steffen, W. Alt, D. Meschede, and A. Widera, *Science* **325**, 174 (2009).